

# Effect of Polyethylene Glycol on the Magnetic Properties of $\gamma$ -Fe<sub>2</sub>O<sub>3</sub> Nanoparticles Synthesized from Fe(III) Carboxylate-Polyethylene Glycol Mixture

A.C. Grigorie, C. Muntean and M. Stefanescu

"Politehnica" University of Timisoara, Faculty of Industrial Chemistry and Environmental Engineering, Bd. V. Parvan Nr. 6, Et. 4, 300223, Timisoara, Romania, e-mail: cornelia.muntean@upt.ro, phone: 004 0256 404164

**Abstract:** This paper presents a new procedure for the obtaining of  $\gamma$ -Fe<sub>2</sub>O<sub>3</sub> nanoparticles as single and well-crystallized phase by thermal treatment at 300 °C.  $\gamma$ -Fe<sub>2</sub>O<sub>3</sub> nanoparticles with an average size of 13 nm were obtained by thermal decomposition of Fe(III) carboxylate-polyethylene glycol mixture. The Fe(III) carboxylate precursor was obtained in the redox reaction between iron nitrate and 1,3-propanediol. Polyethylene glycol (PEG) was used as a coating agent and to limit the agglomeration of  $\gamma$ -Fe<sub>2</sub>O<sub>3</sub> magnetic nanoparticles. The obtaining process of  $\gamma$ -Fe<sub>2</sub>O<sub>3</sub> was studied by thermal analysis and Fourier transform infrared spectroscopy. From thermal behavior of the samples prepared using different Fe(III) carboxylate-PEG molar ratios, it was established 300 °C as annealing temperature. The obtained powder was characterized by X-ray diffractometry, Fourier transform infrared spectroscopy, scanning electron microscopy and magnetic measurements. The resulting  $\gamma$ -Fe<sub>2</sub>O<sub>3</sub> nanoparticles present magnetic properties which are influenced by the PEG amount in the Fe(III) carboxylate-PEG mixture.

**Keywords:** polyethylene glycol,  $\gamma$ -Fe<sub>2</sub>O<sub>3</sub>, magnetic nanoparticles, thermal decomposition

## 1. Introduction

Among the various oxide systems, iron oxides are of great importance in technological and industrial applications [1-3]. Several methods have been developed to synthesize iron oxide nanoparticles [4-6]. Maghemite nanoparticles have been synthesized using a variety of techniques such as laser pyrolysis, co-precipitation [7], sol-gel [8], microemulsion [9], ball-milling [10], and sonochemistry [11].

In the last years, the interest has been focused on the synthesis of  $\gamma$ -Fe<sub>2</sub>O<sub>3</sub> nanoparticles from organic precursors: Fe(acac)<sub>3</sub> [12], Fe(CO)<sub>5</sub> in the presence of residual oxygen of the system [13], Fe-urea complex [Fe(CON<sub>2</sub>H<sub>4</sub>)<sub>6</sub>](NO<sub>3</sub>)<sub>3</sub> [14], a homogeneous solution of stearic acid and hydrated Fe(III) nitrate [15], Fe(III) glyoxylate and succinate [16]. This type of syntheses ensures low temperatures of obtaining, small particles size and a homogeneous distribution of the components at molecular level, as compared to the conventional methods [17].

In our previous works, we used an original synthesis method where carboxylate type precursors are employed for the preparation of simple and mixed oxides [16, 18]. Using the method [19] based on the redox reaction between Fe(III) nitrate and some diols, by thermal decomposition of the synthesized compounds in air at ~300 °C, we obtained single phase  $\gamma$ -Fe<sub>2</sub>O<sub>3</sub> nanoparticles [16]. Using the reactants Fe(NO<sub>3</sub>)<sub>3</sub>·9H<sub>2</sub>O (NO<sub>3</sub><sup>-</sup> anion-oxidizing agent) and polyvinyl alcohol (PVA-reducing agent) at low temperatures,  $\gamma$ -Fe<sub>2</sub>O<sub>3</sub> was also obtained [20].

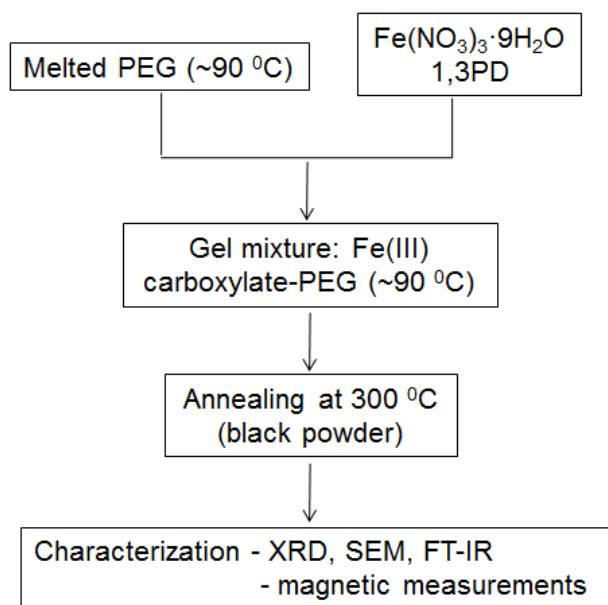
Polyethylene glycol (PEG) is an important biocompatible polymer, widely used as a coating agent for magnetic nanoparticles with various applications in biotechnology. Fe<sub>3</sub>O<sub>4</sub>/PEG magnetic nanocomposite was synthesized via a hydrothermal procedure, where the uniform nanoparticles of Fe<sub>3</sub>O<sub>4</sub> were encapsulated with PEG [21]. The polymer was also used to synthesize nanoparticles by the polyol method, where PEG is a solvent and reducing agent [22].

In this paper, we report the synthesis of  $\gamma$ -Fe<sub>2</sub>O<sub>3</sub> at 300 °C starting from a mixture of iron nitrate-1,3-propanediol and polyethylene glycol with a stabilizing role. The precursor Fe(III) carboxylate was obtained at 90 °C in the redox reaction between iron nitrate and 1,3-propanediol, directly in mixture with PEG. During the synthesis procedure, due to the physico-chemical properties of PEG in mixture with Fe(III) carboxylate,  $\gamma$ -Fe<sub>2</sub>O<sub>3</sub> is formed at the same time with the thermal degradation of the polymer.

## 2. Experimental

The reagents used in the synthesis of  $\gamma$ -Fe<sub>2</sub>O<sub>3</sub> were: iron nitrate Fe(NO<sub>3</sub>)<sub>3</sub>·9H<sub>2</sub>O (M = 404 g mol<sup>-1</sup>), 1,3-propanediol (1,3PD, M = 76 g mol<sup>-1</sup>, ρ = 1.053 g cm<sup>-3</sup>) and polyethylene glycol (PEG, M = 35000 g mol<sup>-1</sup>). All the reagents were of analytical grade and were supplied by Merck.

A schematic representation of the experimental procedure is shown in Fig. 1.

Figure 1. Scheme for experimental procedure of  $\gamma$ - $\text{Fe}_2\text{O}_3$  obtaining

There were synthesized samples (B0, B1 and B2) in different molar ratios (Table 1). The amounts of reagents used in synthesis were calculated to obtain 0.1 g  $\text{Fe}_2\text{O}_3$ .

The required amounts of  $\text{Fe}(\text{NO}_3)_3 \cdot 9\text{H}_2\text{O}$  and stoichiometric diol 1,3PD were mixed with melted PEG (Fig. 1), resulting viscous mixtures. All the samples were submitted to thermal analysis. From the evolution of thermoanalytical curves and Fourier transform infrared (FT-IR) spectra it was highlighted the formation of Fe(III)

carboxylate in mixture with PEG and it was established the decomposition temperature of this mixture.

After annealing at 300 °C, the samples (B0, B1 and B2) were characterized by FT-IR, X-ray diffractometry (XRD), scanning electron microscopy (SEM) and magnetic measurements.

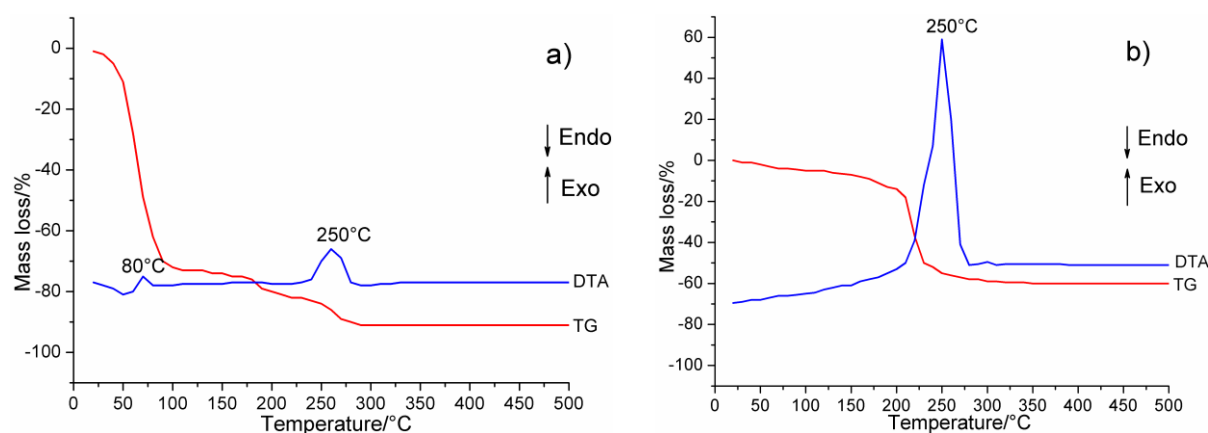
Thermal analysis was performed on a 1500D MOM Budapest derivatograph. Thermogravimetric (TG) and differential thermal analysis (DTA) curves were recorded for 100 mg samples, placed as thin film on Pt plates, at a heating rate of 5 °C  $\text{min}^{-1}$ , in air, up to 500 °C. FT-IR spectra were recorded using a Shimadzu Prestige-21 spectrophotometer in KBr pellets, in the range 400-4000  $\text{cm}^{-1}$ . The phase composition of the powders was determined by XRD using a Rigaku Ultima IV diffractometer, with  $\text{Cu}_{K\alpha}$  radiation ( $\lambda = 1.5418 \text{ \AA}$ ). The samples were annealed at 300 °C for 3 h in a Nabertherm LE 4/11/R6 oven. Particles morphology was investigated by SEM, using a FEI Quanta FEG 250 scanning electron microscope, operating at 30 kV and 7 mm working distance. Magnetic measurements were carried out under quasistatic conditions (50 Hz ac fields) by means of an induction hysteresigraph [23].

### 3. Results and Discussion

Thermoanalytical curves registered to evidence the formation and decomposition of Fe(III) carboxylate are presented in Fig. 2.

TABLE 1. The compositions of  $\text{Fe}(\text{NO}_3)_3 \cdot 9\text{H}_2\text{O}$ -1,3PD-PEG mixtures

Sample	Quantity/mole			% PEG/ $\text{Fe}(\text{NO}_3)_3 \cdot 9\text{H}_2\text{O}$ (mass)
	PEG	$\text{Fe}(\text{NO}_3)_3 \cdot 9\text{H}_2\text{O}$	Diol(1,3PD)	
B0	-	1	1.125	-
B1	0.001	1	1.125	8.03 / 91.97
B2	0.0025	1	1.125	17.90 / 82.10

Figure 2. TG and DTA curves of: a) formation of Fe(III) carboxylate from  $\text{Fe}(\text{NO}_3)_3 \cdot 9\text{H}_2\text{O}$  and 1,3PD and b) decomposition of Fe(III) carboxylate synthesized at 140 °C

From thermoanalytical curves evolution (Fig. 2a), one can observe a weak exothermic effect recorded at 80 °C which is assigned to the redox reaction between  $\text{NO}_3^-$  anion and 1,3PD, when Fe(III) carboxylate is formed, with a mass loss up to 100 °C on TG curve. At 250 °C, on DTA curve is recorded an exothermic effect, corresponding to the oxidative decomposition of the complex combination. Taking into account this information, for the synthesis of Fe(III) carboxylate (with or without PEG), the mixtures corresponding to B0, B1 and B2 samples were heated up to 140 °C. From thermoanalytical curves evolution (Fig. 2b) it is observed that Fe(III) carboxylate synthesized at 140 °C decomposes in the range 200-250 °C, with an exothermic effect recorded on DTA curve. In the range 300-500 °C, the mass remains constant and it corresponds to  $\text{Fe}_2\text{O}_3$ .

In the synthesis conditions, the oxidation of 1,3PD by  $\text{NO}_3^-$  anion takes place at both primary -OH groups that turn into carboxyl groups (-COO), with formation of the malonate dianion ( $\text{C}_3\text{H}_2\text{O}_4^{2-}$ ) according to Eq. (1).

The oxidation of 1,3PD takes place simultaneously with the coordination of the oxidation product to the complex generator ( $\text{Fe}^{3+}$ ). In our previous work it was proposed a structural formula for Fe(III) malonate complex combination [18].

Thermal behavior of  $\text{Fe}(\text{NO}_3)_3 \cdot 9\text{H}_2\text{O}$ -1,3PD-PEG mixtures for the samples synthesized at different ratios (B1 and B2) is presented in Fig. 3.

In the temperature range 50-100 °C, the redox reaction and the melting of PEG (~90 °C) take place, with a weak exothermic effect at 70 °C recorded on DTA curves.

In this range, a mass loss is recorded on TG curves, assigned to the elimination of  $\text{NO}_x$  from redox reaction. The mass loss recorded on TG curves in the range 200-270 °C corresponds to the combustion of PEG and the decomposition of Fe(III) carboxylate, with cumulative exothermic effects. Up to 500 °C, the residual mass remains constant and consists of  $\text{Fe}_2\text{O}_3$  particles and carbon.

FT-IR spectrum of Fe(III) carboxylate-PEG (B1 sample) heated at 140 °C (Fig. 4a) presents the mark of PEG characteristic bands [24] overlapped with  $\nu_{\text{as}}(\text{COO}^-)$  band in the range 1670-1550  $\text{cm}^{-1}$  and  $\nu_{\text{s}}(\text{COO}^-)$  band in the range 1470-1340  $\text{cm}^{-1}$  which proves that Fe(III) carboxylic compound was formed in the mixture.

The viscous gels (B1 and B2 samples) were annealed at 300 °C for 3 h, when the combustion of PEG and the oxidative decomposition of the metal-organic precursors took place with formation of the corresponding  $\text{Fe}_2\text{O}_3$  powders. Fig. 4b presents the FT-IR spectrum of the B1 sample annealed at 300 °C for 3 h. The bands at 637 and 562  $\text{cm}^{-1}$  are assigned to the spinellic  $\gamma\text{-Fe}_2\text{O}_3$  phase [16].

XRD patterns for B0 ( $\text{Fe}(\text{NO}_3)_3 \cdot 9\text{H}_2\text{O}$ -1,3PD) and B2 samples ( $\text{Fe}(\text{NO}_3)_3 \cdot 9\text{H}_2\text{O}$ -1,3PD-PEG) are presented in Fig. 5.

From XRD patterns (Fig.5) one can observe that for both B0 and B2 samples annealed at 300 °C, the lines of a single, well-crystallized phase  $\gamma\text{-Fe}_2\text{O}_3$  are recorded. For B1 sample was recorded a pattern similar to that of B2 sample.

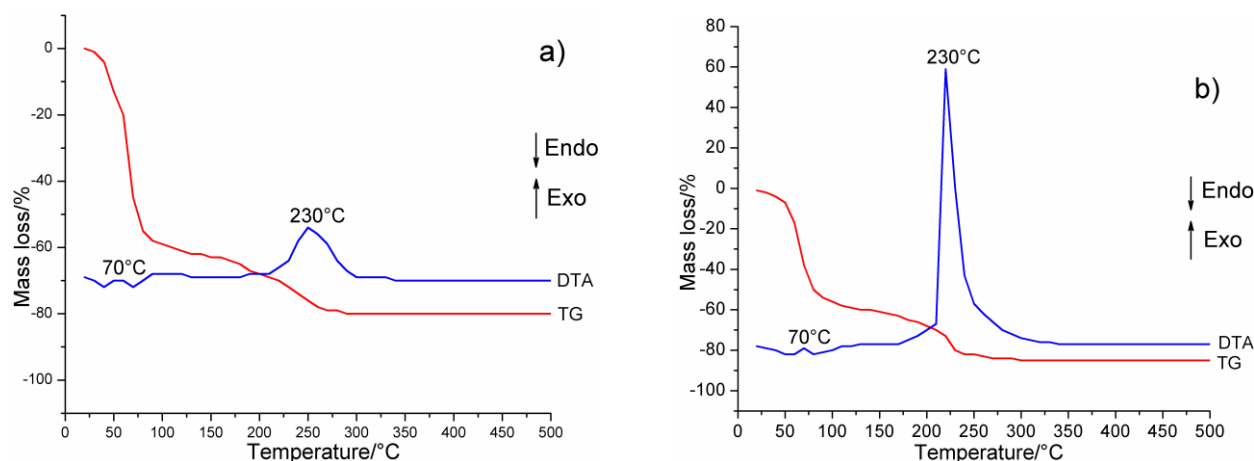
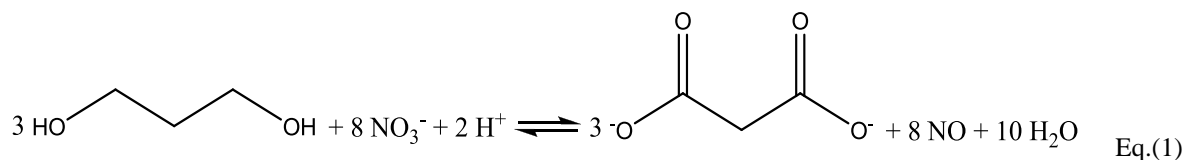


Figure 3. TG and DTA curves of the samples: a) B1 and b) B2

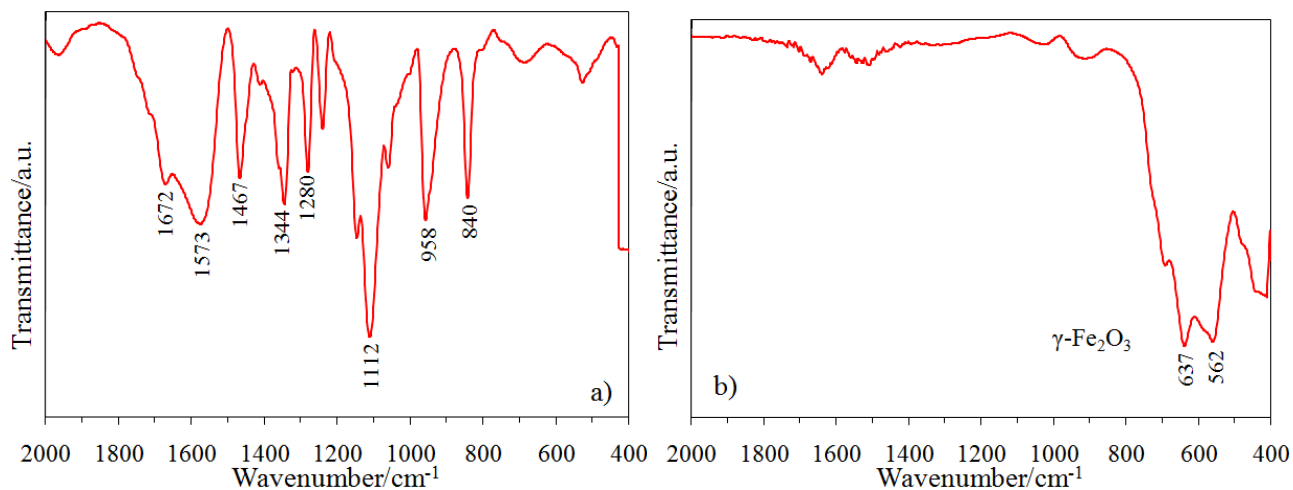


Figure 4. FTIR spectra of: a) B1 sample heated at 140 °C and b) powder obtained at 300 °C

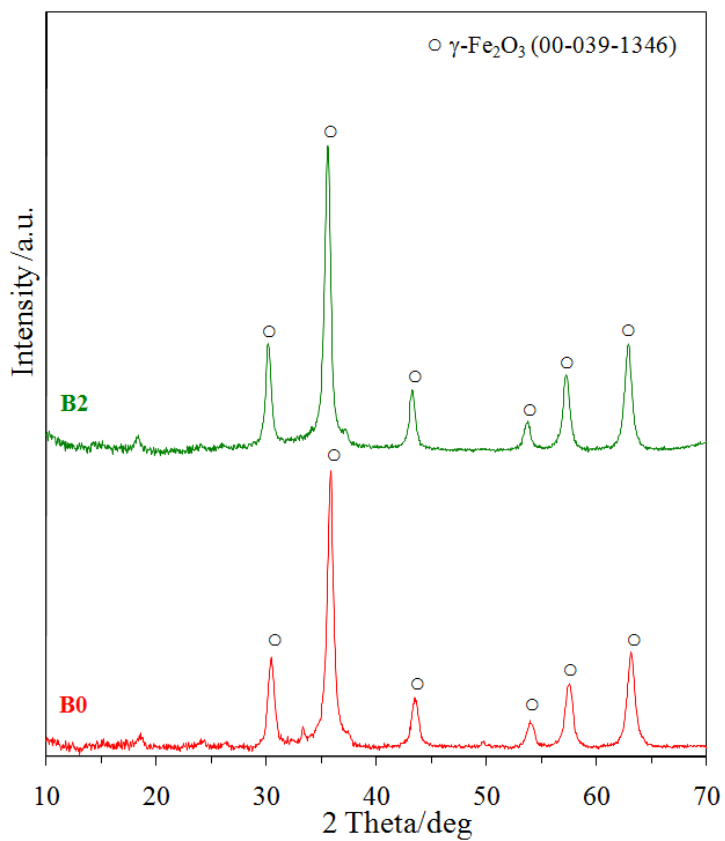


Figure 5. XRD patterns of B0 and B2 samples annealed at 300 °C

Average crystallite size ( $D_{XRD}$ ) of  $\gamma\text{-Fe}_2\text{O}_3$  was calculated based on the Scherrer's equation (2) using the following  $hkl$  peaks: 220, 311 and 551:

$$D_{XRD} = \frac{0.9 \cdot \lambda}{\beta \cdot \cos \theta} \quad (2)$$

where  $D_{XRD}$  is the crystallite size (nm),  $\lambda$  is the radiation wavelength,  $\beta$  is the full width at half of the peak (radians),  $\theta$  is the Bragg angle (degrees) [30].

The lattice parameter of cubic  $\gamma\text{-Fe}_2\text{O}_3$  was calculated based on the X-ray diffraction patterns, using Eq. (3):

$$a = d_{hkl} (h^2 + k^2 + l^2) \quad (3)$$

where  $a$  is the lattice parameter ( $\text{\AA}$ ),  $d$  is the interplanar distance ( $\text{\AA}$ ) and  $hkl$  are the Miller indices of the peaks (220, 311 and 551).

The characteristics of the crystalline phases obtained by annealing of B0, B1 and B2 samples are listed in Table 2.

TABLE 2. Crystallographic data obtained from XRD analysis

Sample	$D_{XRD}/\text{nm}$	$a/\text{\AA}$
B0	12.8	8.3480
B1	12.7	8.3204
B2	14.0	8.3538

The experimental values of the lattice parameters for  $\gamma\text{-Fe}_2\text{O}_3$  for all synthesized samples are very close to that from the literature data ( $\sim 8.33 \text{\AA}$ ) [25, 26].

Fig. 6 presents the SEM images of B1 and B2 samples ( $\gamma\text{-Fe}_2\text{O}_3$ ) annealed at  $300 \text{ }^\circ\text{C}$ . These images show agglomerations of uniform  $\gamma\text{-Fe}_2\text{O}_3$  nanoparticles with a mean diameter of  $\sim 15 \text{ nm}$ , close to the values of mean crystallite size ( $D$ ) given by XRD analysis. It can be observed that the increasing amount of PEG (B2 sample) reduces the agglomeration and prevents the growth of the nanoparticles [27].

The two samples (B1 and B2) with different mass ratios of PEG show a tendency of increasing of the specific magnetization with the increase of PEG content (Fig. 7).

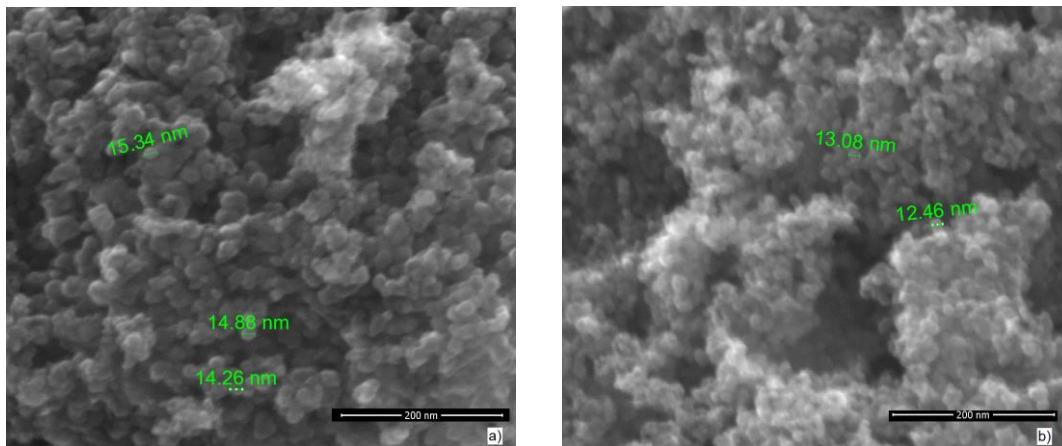


Figure 6. SEM images of  $\gamma\text{-Fe}_2\text{O}_3$  obtained from: a) B1 and b) B2 samples

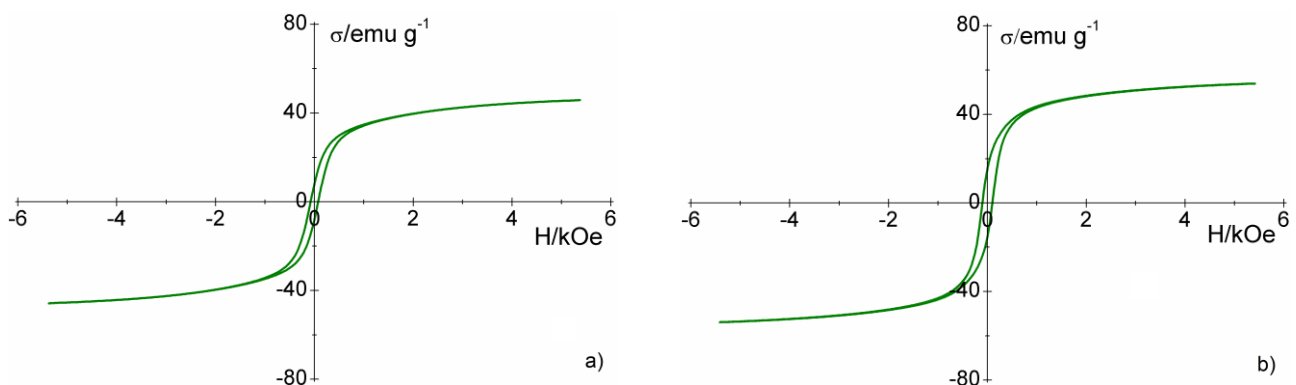


Figure 7. Hysteresis loops of  $\gamma\text{-Fe}_2\text{O}_3$  nanoparticles from: a) B1 and b) B2 samples

The specific saturation magnetization ( $\sigma_s$ ) increases from 48.30 emu g<sup>-1</sup> to 56.37 emu g<sup>-1</sup> and the coercive field ( $H_c$ ) varies from 0.08 to 0.10 kOe when the average crystallites size ( $D_{XRD}$ ) increases from 12.7 nm to 14.0 nm (Table 3). In our previous work it was determined for Fe(NO<sub>3</sub>)·9H<sub>2</sub>O-1,3PD mixture (B0 sample) a specific saturation magnetization of 48.60 emu g<sup>-1</sup> and a coercive field of 0.11 kOe [16]. Thus, one can observe the influence of PEG on the magnetic properties of  $\gamma$ -Fe<sub>2</sub>O<sub>3</sub> nanoparticles. This is due to higher content of carbon particles (B2 sample) that insulates the  $\gamma$ -Fe<sub>2</sub>O<sub>3</sub> magnetic particles. The saturation magnetization of the synthesized  $\gamma$ -Fe<sub>2</sub>O<sub>3</sub> by this method is lower than that of the bulk  $\gamma$ -Fe<sub>2</sub>O<sub>3</sub> (73.5 emu g<sup>-1</sup>) [23, 27].

TABLE 3. Summarized magnetic properties of  $\gamma$ -Fe<sub>2</sub>O<sub>3</sub> nanoparticles

Sample	$D_{XRD}/nm$	$\sigma_s/emu\ g^{-1}$	$H_c/kOe$
B0	12.8	48.60	0.11
B1	12.7	48.30	0.08
B2	14.0	56.37	0.10

#### 4. Conclusions

In the reported study,  $\gamma$ -Fe<sub>2</sub>O<sub>3</sub> nanoparticles were obtained at 300 °C by thermal decomposition of Fe(III) carboxylate-polyethylene glycol mixture. It was observed that PEG acts as a stabilizing agent, limiting the agglomeration of  $\gamma$ -Fe<sub>2</sub>O<sub>3</sub> nanoparticles. The XRD study revealed that by this method  $\gamma$ -Fe<sub>2</sub>O<sub>3</sub> is obtained as nanocrystallites with lattice constant value similar with the one reported in literature. The average crystallite size of  $\gamma$ -Fe<sub>2</sub>O<sub>3</sub> nanoparticles was obtained as ~13 nm. The resulting  $\gamma$ -Fe<sub>2</sub>O<sub>3</sub> nanoparticles present magnetic properties which can be controlled by the PEG amount in Fe(III) carboxylate-PEG mixture. The content of residual carbon resulting from PEG thermal decomposition influences the specific saturation magnetization and the coercive field.

Thermal decomposition of Fe(III) complex combination in mixture with polyethylene glycol is a suitable method for the direct synthesis of  $\gamma$ -Fe<sub>2</sub>O<sub>3</sub> nanoparticles. By changing the amount of PEG it is possible to modify the crystallite size and the magnetic properties of the final product. The obtained  $\gamma$ -Fe<sub>2</sub>O<sub>3</sub> nanoparticles could be considered as a candidate for various applications in magnetic materials area.

#### ACKNOWLEDGEMENT

This work was partially supported by the strategic grant POSDRU/159/1.5/S/137070 (2014) of the Ministry of National Education, Romania, co-financed by the European Social Fund-Investing in People, within the Sectoral Operational Programme Human Resources Development 2007-2013.

#### REFERENCES

1. Yan A., Liu X., Qiu G., Wu H., Yi R., Zhang N. and Xua J., *J. Alloy. Compd.*, 458, **2008**, 487-491.
2. Teng X. and Yang H., *J. Mater. Chem.*, 14, **2004**, 774-779.
3. Shen Y.F., Tang J., Nie Z.H., Wang Y.D., Ren Y. and Zuo L., *Sep. Purif. Technol.*, 68, **2009**, 312-319.
4. Figuerola A., Di Corato R., Manna L. and Pellegrino T., *Pharmacol. Res.*, 62, **2010**, 126-143.
5. He Y., Sahoo Y., Wang S., Luo H., Prasad P.N. and Swihart M.T., *J. Nanopart. Res.*, 8, **2006**, 335-342.
6. Layek S., Pandey A., Pandey A. and Verma H.C., *Int. J. Eng. Sci. Technol.*, 2(8), **2010**, 33-39.
7. Jeong J.R., Lee S.J., Kim J.D. and Shin S.C., *Phys. Stat. Sol.*, 241(7), **2004**, 1593-1596.
8. Chin A.B., Idris Y.I. and Irwan N., *J. Cent. South Univ.*, 20, **2013**, 2954-2959.
9. Tueros M.J., Baum L.A., Borzi R.A., Stewart S.J., Mercader R.C., Marchetti S.G., Bengoa J.F. and Moggi L.V., *Hyperfine Interact.*, 148(1-4), **2003**, 103-108.
10. Burnham P., Dollahon N., Li C.H., Viescas A.J. and Papaefthymiou G.C., *J. Nanopart.*, **2013**, 1-13.
11. Theerdhala S., Alhat D., Vitta S. and Bahadur D., *J. Nanosci. Nanotechnol.*, 8(8), **2008**, 4268-4272.
12. Sun S. and Zeng H., *J. Am. Chem. Soc.*, 124, **2002**, 8204-8205.
13. Woo K., Hong J., Choi S., Lee H., Ahn J. and Kim C.S., *Chem. Mater.*, 16, **2004**, 2814-2818.
14. Asuha S., Zhao S., Wu H.Y., Song L. and Tegus O., *J. Alloys Compd.*, 472, **2009**, 23-25.
15. Deb P. and Bausmalick A., *J. Nanopart. Res.*, 6, **2004**, 527-531.
16. Stefanescu O., Vlase T., Vlase G., Doca N. and Stefanescu M., *Thermochim. Acta*, 519(1-2), **2011**, 22-27.
17. Yue Z., Zhou J., Li L., Zhang H. and Gui Z., *J. Magn. Magn. Mater.*, 208, **2000**, 55-60.
18. Stefanescu O. and Stefanescu M., *J. Organomet. Chem.*, 740, **2013**, 50-55.
19. Birzescu M., Cristea M., Stefanescu M., and Constantin G., *Rom. Pat. 102501*, September 27 **1990**.
20. Stoia M., Tudoran L.B. and Barvinschi P., *J. Therm. Anal. Cal.*, 113(1), **2013**, 11-19.
21. Junejo Y., Baykal A. and Sözeri H., *Cent. Eur. J. Chem.*, 11(9), **2013**, 1527-1532.
22. Tzitzios V., Basina G., Gjoka M., Alexandrakos V., Georgakilas V., Niarchos D., Boukos N. and Petridis D., *Nanotech.*, 17, **2006**, 3750-3755.
23. Mihalca I. and Ercuta A., *J. Optoelectron. Adv. M.*, 5, **2003**, 245-250.
24. Khanna L. and Verma N.K., *Physica B.*, 427, **2013**, 68-75.
25. Sahoo S.K., Agarwal K., Singh A.K., Polke B.G. and Raha K.C., *Int. J. Eng. Sci. Technol.*, 2(8), **2010**, 118-126.
26. Inamdar S.N. and Haram S.K., *J. Nanosci. Nanotechnol.*, 6(7), **2006**, 2155-2158.
27. Honga B. and Qianwang C.T., *Solid State Comm.*, 141, **2007**, 573-576.

Received: 13 November 2014

Accepted: 18 December 2014